Available online at www.sciencedirect.com
SCIENCE DIRECT
Surface Science 600 (2006) 2011–2025
SURFACE SCIENCE
www.elsevier.com/locate/susc

Quasi-chemical approximation for polyatomics: Statistical thermodynamics of adsorption

M. Dávila, F. Romá [1], J.L. Riccardo, A.J. Ramirez-Pastor *

Departamento de Física, Universidad Nacional de San Luis, CONICET, Chacabuco 917, 5700 San Luis, Argentina

Received 6 October 2005; accepted for publication 21 February 2006
Available online 13 March 2006

Abstract

The statistical thermodynamics of interacting polyatomic adsorbates (k-mers) on homogeneous surfaces was developed on a generalization in the spirit of the lattice-gas model and the quasi-chemical approximation (QCA). The new theoretical framework is obtained by combining (i) the exact analytical expression for the partition function of non-interacting linear k-mers adsorbed in one dimension and its extension to higher dimensions, and (ii) a generalization of the classical QCA in which the adsorbate can occupy more than one adsorption site. The coverage and temperature dependence of the Helmholtz free energy, chemical potential, configurational entropy, configurational energy, isosteric heat of adsorption and specific heat are given. The formalism reproduces the classical QCA for monomers, leads to the exact statistical thermodynamics of interacting k-mers adsorbed in one dimension, and provides a close approximation for two-dimensional systems accounting multisite occupancy. Comparisons with analytical data from Bragg–Williams approximation (BWA) and Monte Carlo simulations are performed in order to test the validity of the theoretical model. The resulting thermodynamic description is significantly better than the BWA and still mathematically handable.

Keywords: Lattice-gas models; Multisite occupancy

1. Introduction

The adsorbate–adsorbate interactions in adsorbed films on crystal surfaces have been attracting a great deal of interest since long ago [1–3] and the progress in this field has gained a particular impetu due to their effects on adsorbate structures and chemical reactions on catalyst surfaces, microelectronics fabrication, chemical sensors and electrodes, and surfaces undergoing corrosion [4,5]. Various theories have been proposed to describe monolayer adsorption of interacting particles [1,2]. Particularly, the lattice-gas approximation [1,2,6–8] is one of the most widely used and practically applicable. In this framework, the adsorption field is usually represented by a lattice of adsorption sites.[2] This reduction to simplicity has not only been of academic interest but essential for interpretation of adsorption experiments, determination of gas–solid interaction potentials, and characterization of solid adsorbents.

The introduction of intermolecular forces brings about the possibility of phase transitions [8–11]. Among the common types of phase transitions are, condensation of gases, melting of solids, transitions from paramagnet to ferromagnet and order–disorder transitions. From a theoretical point of view, when nearest-neighbor interactions are present, an extra term in the partition function for interaction energy is required. With this extra term, only partition functions for the whole system can be written. Ising [12] gave an exact solution to the one-dimensional lattice problem in 1925. All other cases are expressed in terms of series

* Corresponding author. Tel.: +54 2652 436151; fax: +54 2652 430224.
E-mail address: antorami@unsl.edu.ar (A.J. Ramirez-Pastor).
[1] Present address: Centro Atómico Bariloche, 8400 San Carlos de Bariloche, Río Negro, Argentina.

[2] Such regular lattice systems with nearest-neighbor interactions are frequently called "Ising models".

0039-6028/$ - see front matter © 2006 Elsevier B.V. All rights reserved.
doi:10.1016/j.susc.2006.02.032

solution [1,13], except for the special case of two-dimensional lattices at half-coverage, which was exactly solved by Onsager [14] in 1944. For the one-dimensional lattice, there is no evidence of phase transitions. Close approximate solutions in dimensions higher than one can be obtained, and the two most important of these are the Bragg–Williams approximation (BWA) [1] and the quasi-chemical approximation (QCA) [1,15]. Both show phase transitions in two-dimensional systems and the BWA incorrectly predicts a phase transition for a linear lattice. These leading models, along with much recent contributions, have played a central role in the study of adsorption systems in presence of lateral interactions between the adatoms. One fundamental feature is preserved in all these theories. This is the assumption that an adsorbed molecule occupies one adsorption site.

In practical situations, most adsorbates involved in adsorption experiments are polyatomic in the sense that, when adsorbed, their typical size is larger than the distance between the nearest-neighbor local minima of the gas–solid potential. For instance, this is true for most *n*-alkanes, *n*-alkenes, cyclic hydrocarbons, etc. [16–19]. However, even the simplest non-spherical molecules such as N_2 and O_2 may adsorb on more than one site depending on the surface structure [20–25]. This effect, so-called multisite occupancy adsorption, introduces a high degree of local correlation in the adsorption theories. Consequently, it has been difficult to formulate, analytically, the statistics of occupation for polyatomics or *k*-mers (particles occupying several *k* contiguous lattice sites). In this sense, exact solutions can be found for special cases, by using Pfaffians [26,27] and the matrix transference method [28,29]. In other words, from an analytical point of view, the problem in which a two-dimensional lattice contains isolated lattice points (vacancies) as well as *k*-mers has not been solved in closed form and approximate methods have been utilized to study this problem.

Three objectives motivated the development of the main approximations existing in the literature, they are (1) to calculate the different ways to array N *k*-mers on a regular lattice of M equivalent sites, $g(M,N)$; (2) to study the influence of surface heterogeneity on the main adsorption properties of polyatomics and (3) the possibility of phase transitions in the adsorbate when nearest-neighbor interacting *k*-mers are adsorbed on homogeneous surfaces. With respect to the first point, several theoretical models have been developed in the past in order to obtain the configurational factor $g(M,N)$. Namely, Flory–Huggins's model [30–32], Guggenheim's model [33], one-dimensional model and extension to higher dimensions [34,35], occupation balance approximation [35], virial expansion [35], etc. In general, these studies can be separated in two groups, according to the shape (or flexibility) of the adsorbate molecule considered: (i) those dealing with flexible *k*-mers [30–32] and (ii) those dealing with linear *k*-mers [33–35]. More recently, a new theory to describe adsorption with multisite occupancy has been introduced [36], which incorporates the configuration of the molecule in the adsorbed state as a model's parameter.

Regarding the point (2), the patchwise heterogeneous surface can be solved relatively simple. One can apply the solution to multisite occupancy adsorption on homogeneous surfaces, which are now the patches. In the case of random heterogeneous surfaces, the problem becomes much more complicated, and it was only two decades ago, when the first solution of that problem was proposed by Nitta et al. [16,37]. Nitta's original approach could be applied only to surfaces characterized by discrete distributions of adsorption energy. Later, Rudziński et al. [16, and references therein] have developed further Nitta's approach to apply also continuous adsorption energy distributions.

Among the theories of the third group, an early seminal contribution is the well-known Flory–Huggins approximation (FHA) [30–32] for binary solutions of polymers molecules diluted in a monomeric solvent (it is worth mentioning that, in the framework of the lattice-gas approach, the adsorption of *k*-mers on homogeneous surfaces is an isomorphous problem to the binary solutions polymer-monomeric solvent). Later, an important contribution to the theoretical study of phase transitions in monolayers of polyatomics has been made by Firpo et al. [38]. Although this model was proposed to describe monolayers of long hydrocarbon chains spread at the gas–liquid interface, its theoretical foundation would remain unchanged if one wanted to apply it to gas–solid systems. In this approach, the configurational factor in the canonical partition function was obtained from the Di Marzio statistics for rigid rod molecules [39]. More recently, Aranovich and Donohue [40] have studied the adsorption of chain molecules by using the Ono and Kondo theory [41]. In all cases, the lateral interactions, which are the responsible of the phase transitions occurring in the adsorbate, were taken into account in the framework of the BWA. A comprehensive discussion on this subject is included in the book of Des Cloiseaux and Janninck [42].

By following this line of reasoning, in recent contributions we reported different models [35,36,43] dealing with adsorption of large molecules. In all cases, the partition function was written as a product of two contributions, the first being the different ways to array N *k*-mers on M homogeneous sites and the second being a term that takes into account the effect of the adsorbate–adsorbate interactions in the framework of the BWA. The present article goes a step further, including the nearest-neighbor interactions by following the configuration-counting procedure of the QCA. For this purpose, a new theoretical formalism is presented based upon (i) the exact analytical expression for the partition function of non-interacting linear *k*-mers adsorbed in one dimension and its extension to higher dimensions [34,35] and (ii) a generalization of the classical QCA in which the adsorbate can occupy more than one adsorption site. In addition, Monte Carlo (MC) simulations are performed in order to test the validity of the theoretical model. The new theoretical scheme allows us (1) to obtain

an approximation that is significantly better than the BWA for polyatomics and, at the same time, mathematically handable; (2) to reproduce the classical QCA for monomers [1] and the exact statistical thermodynamics of interacting k-mers adsorbed in one dimension [44]; (3) to develop an accurate approximation for two-dimensional adlayers accounting multisite occupancy and (4) to provide a simple model from which experiments may be reinterpreted.

The paper is organized as follows: In Section 2, the quasi-chemical approximation for polyatomics is developed. In addition, the basis of the Monte Carlo simulation scheme in the grand canonical and canonical ensembles is given. The results of the theoretical approach are presented in Section 3, along with a comparison with Monte Carlo simulation data corresponding to interacting dimers adsorbed on one-dimensional, honeycomb, square and triangular lattices. Finally, the conclusions are drawn in Section 4.

2. Theory and Monte Carlo simulation

2.1. Quasi-chemical approximation for polyatomics

Here, we address the general case of adsorbates assumed as linear molecules containing k identical units, each of one occupies a lattice site. Small adsorbates with spherical symmetry would correspond to the monomers limit ($k = 1$). The distance between k-mer units is assumed in registry with the lattice constant a; hence exactly k sites are occupied by a k-mer when adsorbed. Two different energies are considered in the adsorption process: (1) U_0, constant interaction energy between a k-mer unit and an adsorption site and (2) w, lateral interaction energy between two nearest-neighbor units belonging to different k-mers. Then, the canonical partition function can be written as [1]

$$Q(N,M,T) = q^N \sum_{N_{11}} g(N,M,N_{11}) \exp[-\beta(wN_{11} + kNU_0)], \tag{1}$$

where q is the partition function for a single adsorbed molecule; M and N represent the number of adsorption sites and adsorbed k-mers, respectively; N_{11} is the number of pairs of nearest-neighbor units belonging to different k-mers; $g(N,\ M,\ N_{11})$ is the number of ways to array N k-mers on M sites with N_{11} pair of occupied sites and $\beta = 1/k_B T$, being k_B the Boltzmann constant.

As it is usual in the case of single-site occupation, it is convenient to write the canonical partition function as a function of N_{01}, being N_{01} the number of pairs formed by an empty site adjacent to a occupied site. For this purpose, we calculate the relations between N_{11}, N_{01} and N_{00} (being N_{00} the number of pairs of empty nearest-neighbor sites):

$$2N_{11} + N_{01} + 2N(k-1) = ckN, \tag{2}$$

$$2N_{00} + N_{01} = c(M - kN), \tag{3}$$

where "number of 01 pairs" = "number of 10 pairs" = $N_{01}/2$ and c is the coordination number of the lattice. In the case of $k = 1$, the well-known relations for single-site occupation are recovered [1].

Now, the canonical partition function can be written in terms of N_{01}

$$Q(N,M,T) = q^N \exp\{-\beta N[\lambda w/2 + kU_0]\} \times \sum_{N_{01}} g(N,M,N_{01}) \exp(\beta w N_{01}/2) \tag{4}$$

and $\lambda = (c-2)k + 2$.

By using the standard formalism of the QCA, the number of ways of assigning a total of $[cM/2 - N(k-1)]$ independent pairs[3] to the four categories 11, 10, 01, and 00, with any number 0 through $[cM/2 - N(k-1)]$ per category consistent with the total, is

$$\tilde{g}(N,M,N_{01}) = \frac{[cM/2 - N(k-1)]!}{[(N_{01}/2)!]^2 [c(M-kN)/2 - N_{01}/2]! [\lambda N/2 - N_{01}/2]!}. \tag{5}$$

This cannot be set equal to $g(N,M,N_{01})$ in Eq. (4), because treating the pairs as independent entities leads to some unphysical configurations (see Ref. [1, p. 253]). Thus $\tilde{g}$ overcounts the number of configurations. To take care of this, we must normalize $\tilde{g}$

$$g(N,M,N_{01}) = C(N,M)\ \tilde{g}(N,M,N_{01}) \tag{6}$$

and

$$g(N,M) = \sum_{N_{01}} g(N,M,N_{01}) = C(N,M) \sum_{N_{01}} \tilde{g}(N,M,N_{01}), \tag{7}$$

where $g(N,M)$ is number of ways to arrange N k-mers on M sites. In general, $g(N,M)$ depends on the spatial configuration of the k-mer and the surface geometry. Even in the simplest case of linear k-mers, there not exist the exact form of $g(N,M)$ in two (or more) dimensions.[4] However, different approximations have been developed for $g(N,M)$ [35], which allow us to obtain $C(N,M)$.

In order to calculate $C(N,M)$, we replace $\sum_{N_{01}} \tilde{g}(N,M,N_{01})$ by the maximum term in the sum, $\tilde{g}(N,M,N_{01}^*)$. By taking logarithm in Eq. (5), using the Stirling's approximation and operating, it results

$$\begin{aligned}\ln \tilde{g}(N,M,N_{01}) &= [cM/2 - (k-1)N] \ln[cM/2 - (k-1)N] - N_{01} \ln N_{01}/2 \\ &\quad - [c(M-kN)/2 - N_{01}/2] \ln[c(M-kN)/2 - N_{01}/2] \\ &\quad - (\lambda N/2 - N_{01}/2) \ln(\lambda N/2 - N_{01}/2).\end{aligned} \tag{9}$$

[3] The term $N(k-1)$ is subtracted since the total number of nearest-neighbor pairs, $cM/2$, includes the $N(k-1)$ bonds belonging to the N adsorbed k-mers.

[4] In the case $c = 2$ (one-dimensional lattice), it is possible to write [34],

$$g(N,M) = \frac{[M-(k-1)N]!}{N!(M-kN)!}, \tag{8}$$

which is an exact result.

By differentiating the last equation with respect to N_{01}

$$\tilde{g}'(N,M,N_{01}) = \frac{\tilde{g}(N,M,N_{01})}{2}\ln\left\{\frac{[c(M-kN)-N_{01}](\lambda N-N_{01})}{N_{01}^2}\right\}. \quad (10)$$

Setting $\tilde{g}'(N,M,N_{01})=0$ and solving for N_{01}^*, the value of N_{01} in the maximum term of $\tilde{g}$,

$$N_{01}^* = \frac{c\lambda N(M-kN)}{cM-2(k-1)N} = \lambda N - \frac{\lambda^2 N^2}{cB} \quad (11)$$

and

$$B = M - 2(k-1)N/c. \quad (12)$$

Then,

$$\tilde{g}(N,M,N_{01}^*) = \frac{(cB/2)!}{\left[\left(\lambda N/2-\frac{\lambda^2N^2}{2cB}\right)!\right]^2\left(cB/2-\lambda N+\frac{\lambda^2N^2}{2cB}\right)!\left(\frac{\lambda^2N^2}{2cB}\right)!}, \quad (13)$$

and, by simple algebra,

$$\tilde{g}(N,M,N_{01}^*) = \left[\frac{B!}{(B-\lambda N/c)!(\lambda N/c)!}\right]^c. \quad (14)$$

Eq. (14) allows us to calculate $C(N,M)$,

$$C(N,M) = \frac{g(N,M)}{\tilde{g}(N,M,N_{01}^*)} = g(N,M)\left[\frac{(B-\lambda N/c)!(\lambda N/c)!}{B!}\right]^c. \quad (15)$$

Now, $\ln Q(N,M,T)$ [see Eq. (4)] can be written as

$$\ln Q(N,M,T) = N\ln q - \beta N[\lambda w/2 + kU_0] + \ln\left\{\sum_{N_{01}} C(N,M)\tilde{g}(N,M,N_{01})\exp(\beta w N_{01}/2)\right\}. \quad (16)$$

As in Eq. (7), we replace $\sum_{N_{01}} C(N,M)\tilde{g}(N,M,N_{01})\exp(\beta w N_{01}/2)$ by the maximum term in the sum, $C(N,M)\tilde{g}(N,M,N_{01}^{**})\exp(\beta w N_{01}^{**}/2)$. Thus,

$$C(N,M)\tilde{g}'(N,M,N_{01}^{**})\exp(\beta w N_{01}^{**}/2) + C(N,M)\tilde{g}(N,M,N_{01}^{**})\exp(\beta w N_{01}^{**}/2)\beta w/2 = 0, \quad (17)$$

then,

$$\frac{\tilde{g}'(N,M,N_{01}^{**})}{\tilde{g}(N,M,N_{01}^{**})} = -\beta w/2. \quad (18)$$

From Eqs. (10) and (18),

$$(cB-\lambda N-N_{01}^{**})(\lambda N-N_{01}^{**}) = {N_{01}^{**}}^2\exp(-\beta w) \quad (19)$$

and

$$[1-\exp(-\beta w)]{N_{01}^{**}}^2 - cBN_{01}^{**} + (cB-\lambda N)\lambda N = 0. \quad (20)$$

Solving Eq. (20) we obtain[5]

$$\frac{N_{01}^{**}}{cB} = \frac{1-\sqrt{1-4A(1-\lambda N/cB)(\lambda N/cB)}}{2A}, \quad (21)$$

where $A = 1-\exp(-\beta w)$.

Finally, the canonical partition function can be written in terms of N_{01}^{**},

$$Q(N,M,T) = q^N\exp\{-\beta N[\lambda w/2 + kU_0]\}g(N,M) \times\left[\frac{(B-\lambda N/c)!(\lambda N/c)!}{B!}\right]^c\tilde{g}(N,M,N_{01}^{**}) \times\exp(\beta w N_{01}^{**}/2). \quad (22)$$

In this work, we will use the following expression for $g(N,M)$:

$$g(N,M) = K(c,k)^N\frac{(B-\lambda N/c+N)!}{N!(B-\lambda N/c)!}, \quad (23)$$

which is an extension to two dimensions of the exact configurational factor obtained in one dimension [35]. $K(c,k)$ is, in general, a function of the connectivity and the size of the molecules. In the particular case of rigid straight k-mers, the simplest approximation provides $K(c,k) = c/2$.

Introducing Eq. (23) in Eq. (22), taking logarithm and using the Stirling's approximation, it results

$$\begin{aligned}\ln Q(N,M,T) &= N\ln q - \beta N[\lambda w/2 + kU_0] + N\ln K(c,k)\\ &+ \beta w N_{01}^{**}/2 + (B-\lambda N/c+N)\ln(B-\lambda N/c+N)\\ &- N\ln N + (c-1)(B-\lambda N/c)\ln(B-\lambda N/c)\\ &+ \lambda N\ln\lambda N/c - cB\ln B\\ &+ cB/2\ln cB/2 - N_{01}^{**}\ln N_{01}^{**}/2\\ &- (cB/2-\lambda N/2-N_{01}^{**}/2)\\ &\times\ln(cB/2-\lambda N/2-N_{01}^{**}/2)\\ &- (\lambda N/2-N_{01}^{**}/2)\ln(\lambda N/2-N_{01}^{**}/2). \end{aligned} \quad (24)$$

From Eq. (24), the Helmholtz free energy per site, $f(N,M,T) = F(N,M,T)/M$ [being $\beta F(N,M,T) = -\ln Q(N,M,T)$], can be obtained as a function of surface coverage, $\theta = kN/M$, and temperature,

$$\begin{aligned}\beta f(\theta,T) &= -\frac{\theta}{k}\ln qK(c,k) + \beta w\left(\frac{\lambda\theta}{2k}-\alpha\right)\\ &- \left[\frac{c}{2}-\left(\frac{k-1}{k}\right)\theta\right]\ln\left\{\frac{\left[1-\left(\frac{k-1}{k}\right)\theta\right]^{2/c}(1-\theta)^{2(c-1)/c}\left[\frac{c}{2}-\left(\frac{k-1}{k}\right)\theta\right]}{\left[1-\frac{2}{c}\left(\frac{k-1}{k}\right)\theta\right]^2\left[\frac{c}{2}(1-\theta)-\alpha\right]}\right\}\\ &- \frac{\theta}{k}\ln\left\{\frac{\left(\frac{\lambda\theta}{ck}\right)^{\lambda}\left[\frac{c}{2}(1-\theta)-\alpha\right]^{\lambda/2}}{\frac{\theta}{k}\left[1-\left(\frac{k-1}{k}\right)\theta\right]^{(\lambda-c)/c}(1-\theta)^{(\lambda c-\lambda)/c}\left[\frac{\lambda\theta}{2k}-\alpha\right]^{\lambda/2}}\right\}\\ &- 2\alpha\ln\left\{\frac{\left[\frac{c}{2}(1-\theta)-\alpha\right]^{1/2}\left[\frac{\lambda\theta}{2k}-\alpha\right]^{1/2}}{\alpha}\right\}, \end{aligned} \quad (25)$$

where α is

$$\alpha = \frac{N_{01}^{**}}{2M} = \frac{\lambda c}{2k}\frac{\theta(1-\theta)}{\left[\frac{c}{2}-\left(\frac{k-1}{k}\right)\theta+b\right]} \quad (26)$$

[5] The solution $N_{01}^{**}/cB = (1+\sqrt{\cdots})/2A$ is discarded for physical reasons.

and

$$b = \left\{ \left[\frac{c}{2} - \left(\frac{k-1}{k} \right) \theta \right]^2 - \frac{\lambda c}{k} A\theta(1-\theta) \right\}^{1/2}. \tag{27}$$

The equilibrium properties of the adlayer can be deduced from Eq. (24) along with the differential form of F in the canonical ensemble

$$\mathrm{d}F = -S\mathrm{d}T - \Pi \mathrm{d}M + \mu \mathrm{d}N, \tag{28}$$

where S, Π and μ represent the entropy, the spreading pressure and the chemical potential, respectively.

Thus, the coverage dependence of the chemical potential, $\mu[=(\partial F/\partial N)_{M,T}]$, arises straightforwardly from Eqs. (24) and (28)

$$K(c,k)\left(\frac{2}{c}\right)^{2(k-1)} \exp[\beta(\mu - w\lambda/2)] = \frac{\theta}{k} \frac{(1-\theta)^{k(c-1)}[k-(k-1)\theta]^{k-1}\left[\frac{\lambda\theta}{2k} - \alpha\right]^{\lambda/2}}{\left[\frac{ck}{2} - (k-1)\theta\right]^{k-1}\left[\frac{c}{2}(1-\theta) - \alpha\right]^{kc/2}\left(\frac{\lambda\theta}{ck}\right)^{\lambda}}. \tag{29}$$

The configurational energy per site, u, can be calculated as

$$u = w\frac{N_{01}^{**}}{M} = w\left(\frac{\lambda N}{2M} - \frac{N_{01}^{**}}{2M}\right) = w\left(\frac{\lambda\theta}{2k} - \alpha\right). \tag{30}$$

In addition, $f = u - Ts$ and the entropy per site, s, can be obtained from Eqs. (25) and (30) as

$$\begin{aligned} \frac{s}{k_B} = {} & \frac{\theta}{k}\ln qK(c,k) \\ & + \left[\frac{c}{2} - \left(\frac{k-1}{k}\right)\theta\right] \ln\left\{ \frac{\left[1 - \left(\frac{k-1}{k}\right)\theta\right]^{2/c}(1-\theta)^{2(c-1)/c}\left[\frac{c}{2} - \left(\frac{k-1}{k}\right)\theta\right]}{\left[1 - \frac{2}{c}\left(\frac{k-1}{k}\right)\theta\right]^2\left[\frac{c}{2}(1-\theta) - \alpha\right]} \right\} \\ & + \frac{\theta}{k}\ln\left\{ \frac{\left(\frac{\lambda\theta}{ck}\right)^{\lambda}\left[\frac{c}{2}(1-\theta) - \alpha\right]^{\lambda/2}}{\frac{\theta}{k}\left[1 - \left(\frac{k-1}{k}\right)\theta\right]^{(\lambda-c)/c}(1-\theta)^{(\lambda c-\lambda)/c}\left[\frac{\lambda\theta}{2k} - \alpha\right]^{\lambda/2}} \right\} \\ & + 2\alpha\ln\left\{ \frac{\left[\frac{c}{2}(1-\theta) - \alpha\right]^{1/2}\left[\frac{\lambda\theta}{2k} - \alpha\right]^{1/2}}{\alpha} \right\}. \end{aligned} \tag{31}$$

The isosteric heat of adsorption q_{st} is defined as [2]

$$\left(\frac{\partial\beta\mu}{\partial T}\right)_{\theta} = \frac{q_{st}}{k_B T^2}, \tag{32}$$

which can be calculated explicitly from Eq. (29):

$$q_{st}(\theta,T) = -\frac{\lambda w}{2} + \left\{ \frac{\lambda}{2}\left(\frac{\lambda\theta}{2k} - \alpha\right)^{-1} - \frac{kc}{2}\left[\frac{c}{2}(1-\theta) - \alpha\right]^{-1} \right\} \frac{w\alpha^2\exp(-\beta w)}{b}. \tag{33}$$

Finally, the heat capacity per site, c_v, results

$$\frac{c_v}{k_B} = \frac{1}{k_B}\frac{\partial u}{\partial T} = (\beta w\alpha)^2 \frac{\exp(-\beta w)}{b}. \tag{34}$$

2.2. Monte Carlo simulation scheme

MC simulations were used in order to test the applicability of the new theoretical proposition. The system chosen for the comparison was a lattice-gas of interacting dimers,[6] whose Hamiltonian can be written as

$$H = w\sum_{\langle i,j\rangle} c_i c_j - Nw + U_0 \sum_i c_i, \tag{35}$$

where $\langle i,j\rangle$ represents pairs of nearest-neighbor sites and c_i is the occupation variable, which can take the following values: $c_i = 0$ if the corresponding site is empty and $c_i = 1$ if the site is occupied. The term Nw is subtracted in Eq. (35) since the summation over all the pairs of nearest-neighbor sites overestimates the total energy by including N bonds belonging to the N adsorbed dimers. In the simulations, U_0 is set equal zero, without any lost of generality.

The adsorption isotherm, configurational energy and isosteric heat of adsorption are simulated through a grand canonical ensemble Monte Carlo (GCEMC) method [45–47], using Glauber's dynamics. The procedure is as follows. For a given value of the temperature T and chemical potential μ, an initial configuration with N dimers adsorbed at random positions (on $2N$ sites) is generated. Then an adsorption–desorption process is started, where a pair of nearest-neighbor sites is randomly chosen and a random number $\xi \in [0,1]$ is generated:

(1) If the two sites are empty then adsorb a molecule if $\xi \leqslant W$.
(2) If the two sites are occupied by atoms belonging to the same molecule then desorb the molecule if $\xi \leqslant W$.
(3) Otherwise, the attempt is rejected.

W is the transition probability given by the Metropolis [48] rule.

A Monte Carlo Step (MCS) is achieved when M pair of sites have been tested to change its occupancy state. The equilibrium state can be well reproduced after discarding the first $m' = 10^5$–10^6 MCS. Then, averages are taken over $m = 10^5 - 10^6$ successive configurations.

Thermodynamic quantities, such as mean coverage, $\theta = 2\langle N\rangle/M$, and configurational energy, $U = \langle H\rangle$, are obtained as simple averages. In the case of isosteric heat of adsorption, more calculations are required [49,46],

$$q_{st} = -\frac{\partial\langle H\rangle}{\partial\langle N\rangle} = -\frac{\langle HN\rangle - \langle H\rangle\langle N\rangle}{\langle N^2\rangle - \langle N\rangle^2}, \tag{36}$$

where $\langle HN\rangle$, $\langle H\rangle$, $\langle N\rangle$ and $\langle N^2\rangle$ can be evaluated via GCEMC.

On the other hand, heat capacity per site and configurational entropy per site are calculated by using a standard importance sampling Monte Carlo method in the canonical

[6] The dimer is the simplest case of a polyatomic adsorbate and contains all the properties of the multisite occupancy adsorption.

ensemble (CEMC) [45–47]. The thermodynamic equilibrium is reached by following Kawasaki's dynamics, generalized to deal with polyatomic molecules [50]. In this scheme, a dimer and a pair of nearest-neighbor empty sites are randomly selected, and their positions are established. Then, an attempt is made to interchange its occupancy state with probability given by the Metropolis rule [48]. The approximation to thermodynamical equilibrium is usually reached in 10^6 MCS. After that, mean values of the adsorption energy U (at constant coverage and temperature), are obtained by simple averages over 10^6 MCS configurations.

The heat capacity results

$$\frac{c_v}{k_B} = \frac{1}{M}\frac{\langle H^2\rangle - \langle H\rangle^2}{k_B T^2}, \tag{37}$$

where $\langle H\rangle$ and $\langle H^2\rangle$ are evaluated via CEMC.

The configurational entropy s of the adsorbate cannot be directly computed. To calculate entropy, various methods have been developed [47]. Among them, the thermodynamic integration method is one of the most widely used and practically applicable. The method in the CEMC relies upon integration of the configurational energy on temperature along a reversible path between an arbitrary reference state and the desired state of the system. In addition, in order to obtain the entropy of a given state, the entropy of a reference state must be known. Thus, for a system made of N particles on M lattice sites at temperature T, we have

$$\left(\frac{\partial S}{\partial T}\right)_{N,M} = \frac{1}{T}\left(\frac{\partial U}{\partial T}\right)_{N,M} \tag{38}$$

it follows

$$S(N,M,T) = S(N,M,\infty) + \int_{\infty}^{T}\frac{\mathrm{d}U}{T}. \tag{39}$$

The last equation allows to calculate the entropy in different equilibrium states if $S(N,M,\infty)$ (reference state) is known, given that the integral in the second term can be accurately estimated by evaluating U for various values of T following the standard procedure of CEMC. Then, $U(T)$ is spline-fitted and numerically integrated [51,52]. The entropy in the reference state is obtained by using the artificial Hamiltonian method [51,52].

3. Results and discussion

In the present section, we will analyze the main characteristics of the thermodynamic functions given in Eqs. (29) and (34), in comparison with simulation results for a lattice-gas of interacting dimers on one-dimensional, honeycomb, square and triangular lattices.

The computational simulations have been developed for one-dimensional chains of 10^4 sites, and honeycomb, square and triangular $L\times L$ lattices, with $L = 144$, 144 and 150, respectively, and periodic boundary conditions. With this lattice size we verified that finite-size effects are negligible. Note, however, that the linear dimension L has to be properly chosen such that the adlayer structure is not perturbed.

For comparison purposes, it is instructive to begin by discussing the behavior of the one-dimensional case (Figs. 1–4), where two k-mers interact through their ends with an interaction energy that amounts w when the ends are nearest-neighbors. In this case, Eqs. (29) and (34) reduce to the rigorous functions of interacting chains adsorbed flat on a one-dimensional lattice [44]. From the experimental point of view, the adsorption potential within the narrowest nanotubes can be matched to a homogeneous one-dimensional lattice of adsorption sites. It has also been

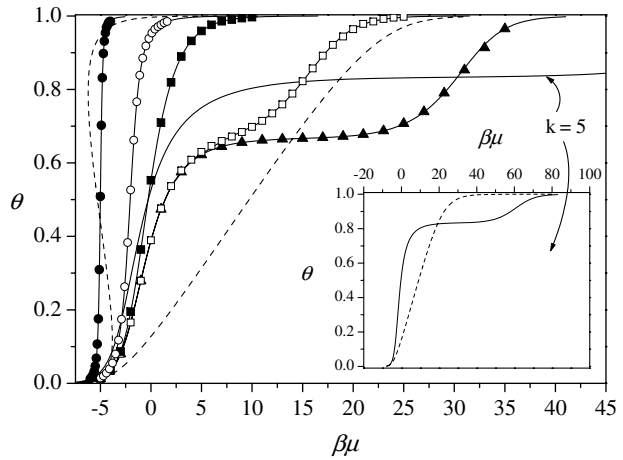

Fig. 1. Lattice coverage θ versus relative chemical potential $\beta\mu$ for interacting (repulsive as well attractive) dimers and 5-mers. Solid lines correspond to QCA and symbols represent results from Monte Carlo simulation: full circles, $k = 2$, $\beta w = -5$; open circles, $k = 2$, $\beta w = -2$; full squares, $k = 2$, $\beta w = 0$; open squares, $k = 2$, $\beta w = +5$; and full triangles, $k = 2$, $\beta w = +10$. In the limit cases ($\beta w = -5$ and $\beta w = 10$), the data are compared with BWA (dashed lines). Inset: Comparison between QCA and BWA for $k = 5$ and $\beta w = +10$.

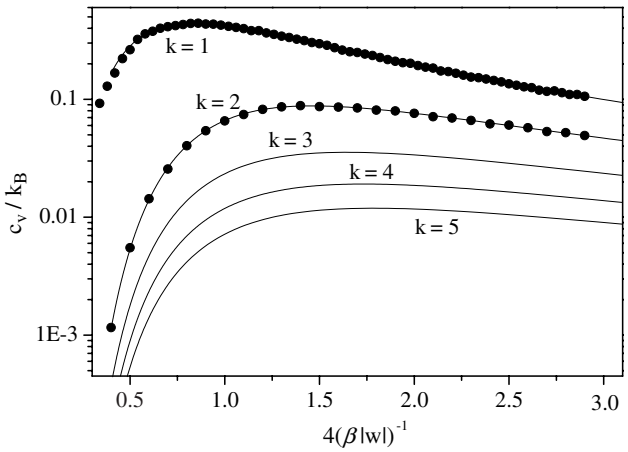

Fig. 2. Specific heat in units of k_B (in log scale) versus $4(\beta|w|)^{-1}$ at $\theta = 0.5$. Monomers ($k = 1$); dimers ($k = 2$); trimers ($k = 3$); tetramers ($k = 4$) and pentamers ($k = 5$). The symbols (full circles) represent results from Monte Carlo simulations.

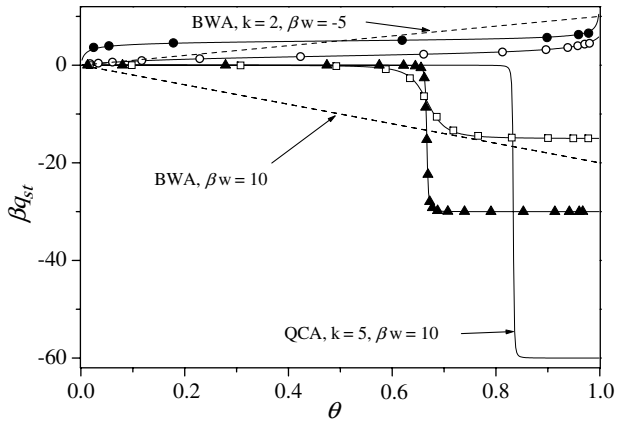

Fig. 3. As Fig. 1 for the isosteric heat of adsorption in $k_B T$ units, βq_{st}, versus lattice coverage.

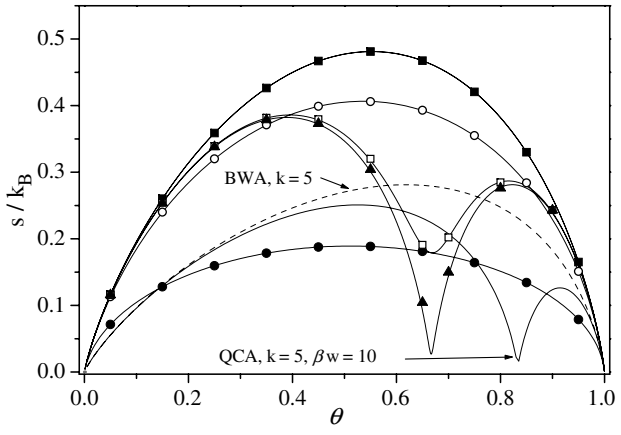

Fig. 4. Entropy per site in units of k_B, s/k_B, versus lattice coverage, θ; the curves correspond one-to-one to the cases displayed in Fig. 1.

reported the one-dimensional character of adsorption in grooves of surface crystal planes of TiO_2 [53].

The coverage dependence of the chemical potential (adsorption isotherm) is shown in Fig. 1 for various k-mer's sizes and interaction energies [attractive ($w < 0$) as well as repulsive ($w > 0$)]. As it is expected, MC simulations in the grand canonical ensemble (symbols) fully agree with the predictions from QCA (solid lines).

For attractive interactions, isotherms shift to lower values of $\beta\mu$ and their slope increases as the ratio βw increases. Qualitatively, no significant changes are observed as the k-mer size increases. However, the curves have a pronounced plateau at $\theta = k/(k+1)$ for strongly repulsive interactions, which smoothes out for already $\beta w = +2$. It is worth noticing that although the double-steep isotherm may be indicative of a second-order phase transition, it is well known that no phase transition develops in a one-dimensional lattice when weak coupling between neighboring particles exists. This is clearly seen in Fig. 2 where the smooth dependence of the specific heat on temperature is depicted for various k-mers at $\theta = 0.5$. A continuum variation of c_v/k_B on T is observed with a maximum that lowers and broadens as the k-mers size increases.

In this case, the plateau in the adsorption isotherm arises along with rearrangement of the adsorbate molecules within the chain. This behavior can be better understood from the curves of the isosteric heat of adsorption in Fig. 3. Thus, q_{st} is nearly zero for coverage $\theta < k/(k+1)$, since the adsorbed particles can rest separated by more or at least one empty site in this regime. Adsorption of a k-mer for $\theta > k/(k+1)$ requires to create a chain of k empty sites, therefore $k-1$ particles must be forced to new positions becoming nearest-neighbors. The resulting energy change for such process is given by the factor $(k-1)w$ (because of the referred rearrangement of the $k-1$ molecules), plus $2w$ coming from the interaction of the adsorbed k-mer with its neighbors. The value of the differential heat at coverage $\theta > k/k+1$ is $q_{st} = -[2w + (k-1)w]$.

The limit cases in Figs. 1 and 3 are compared with results from a mean-field approach, based on BWA. In this framework, the isotherm equation and isosteric heat of adsorption take the form [44,1]

$$K(c,k)k\exp[\beta(\mu - \lambda w\theta)] = \frac{\theta\left[1 - \frac{(k-1)}{k}\theta\right]^{(k-1)}}{(1-\theta)^k} \tag{40}$$

and

$$q_{st}(\theta) = -\lambda w\theta, \tag{41}$$

respectively.

In the attractive case ($\beta w = -5$), a characteristic van der Waals loop is observed in the adsorption isotherm and BWA incorrectly predicts a phase transition for $c = 2$. For strong repulsive couplings ($\beta w = 10$), the BWA curves apart from the exact results and does not reproduce the plateau in the adsorption isotherm. In addition, the isosteric heat of adsorption does not depend on k.

The limitations of the BWA can be much easily visualized with the help of the entropy per site (see Fig. 4). In fact, the main assumption of the BWA say that the configurational degeneracy and average nearest-neighbor interaction energy are treated as though the molecules were distributed randomly among the sites. Consequently, the entropy per site does not depend on w and adopts the form

$$\frac{s(\theta)}{k_B} = \left[1 - \frac{k-1}{k}\theta\right]\ln\left[1 - \frac{k-1}{k}\theta\right] - \frac{\theta}{k}\ln\frac{\theta}{k} - (1-\theta)\ln(1-\theta) + \frac{\theta}{k}\ln K(c,k). \tag{42}$$

Eq. (42) is equivalent to giving all configurations of N k-mers on M sites the same weight as they would have $w = 0$. This situation is clearly reflected in Fig. 4.

The results in Figs. 1–4 allow us to validate the MC scheme. Hereafter, we present the analysis of the adsorption thermodynamics of interacting k-mers on two dimensions.

Typical adsorption isotherms obtained by MC simulations in the grand canonical ensemble (symbols) and comparison with QCA (solid lines) and BWA (dashed lines) are shown in Figs. 5–7, for honeycomb, square and triangular lattices, respectively.

For attractive interactions (Figs. 5(a), 6(a) and 7(a)), as the temperature decreases, the system undergoes a first-order phase transition that shows as the discontinuity in the simulated isotherms and as the typical loops in the theoretical isotherms. In this situation, which has been observed experimentally in numerous systems [2,8], the only phase which one expects is a lattice-gas phase at low coverage, separated by a two-phase coexistence region from a ''lattice-fluid'' phase at higher coverage. This lattice-fluid can be considered as a version of the registered (1×1) phase (where every available site of the lattice is occupied) diluted with vacancies.

This condensation of a two-dimensional gas to a two-dimensional liquid is similar to that of a lattice-gas of attractive monomers. However, the symmetry particle-vacancy (valid for monoatomic particles) is broken for k-mers and the isotherms are asymmetric with respect to $\theta = 0.5$.

The isotherms in the repulsive case (Figs. 5(b), 6(b) and 7(b)) have more features because of the existence of ordered structures in the adlayer. These structures are clearly evidence of subcritical behavior (the systems undergoes continuous phase transitions, from disorder to ordered structures [54,55]). At high temperatures, the isotherms do not present any peculiar behavior. For low temperatures, we can see the typical steps which correspond to the developing of some ordered phase structures and the shape of the isotherms is much dependent on the connectivity. In fact, as the chemical potential μ increases and θ varies from 0 to 1, we found two different ordered phases in

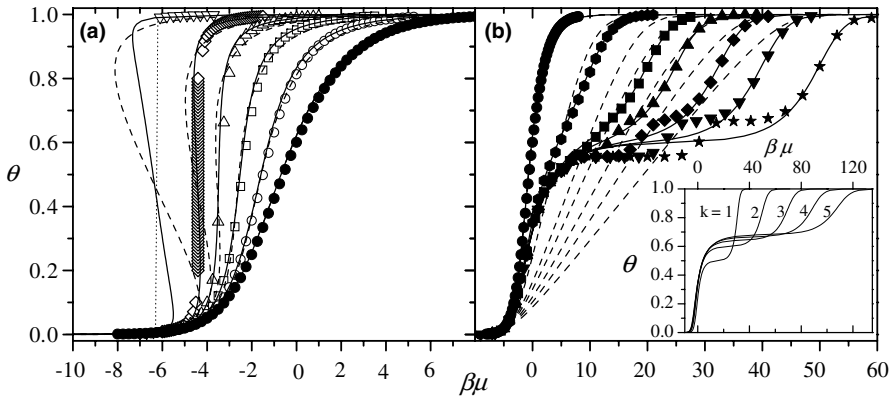

Fig. 5. Adsorption isotherms for homonuclear dimers adsorbed on a honeycomb lattice with nearest-neighbor interactions. Symbols, solid lines and dashed lines represent results from Monte Carlo simulations, QCA and BWA, respectively. The dotted lines are included in the figure as a guide for the eyes. (a) Attractive case: full circles, $\beta w = 0$; open circles, $\beta w = -0.5$; open squares, $\beta w = -1.0$; open up triangles, $\beta w = -1.5$; open diamonds, $\beta w = -2.0$ and open down triangles, $\beta w = -3.0$. (b) Repulsive case: full circles, $\beta w = 0$; full hexagons, $\beta w = 2.0$; full squares, $\beta w = 4.0$; full up triangles, $\beta w = 5.0$; full diamonds, $\beta w = 6.5$; full down triangles, $\beta w = 8.0$ and full stars, $\beta w = 10.0$. Inset: Adsorption isotherms from QCA for $\beta w = 10.0$ and different values of k as indicated.

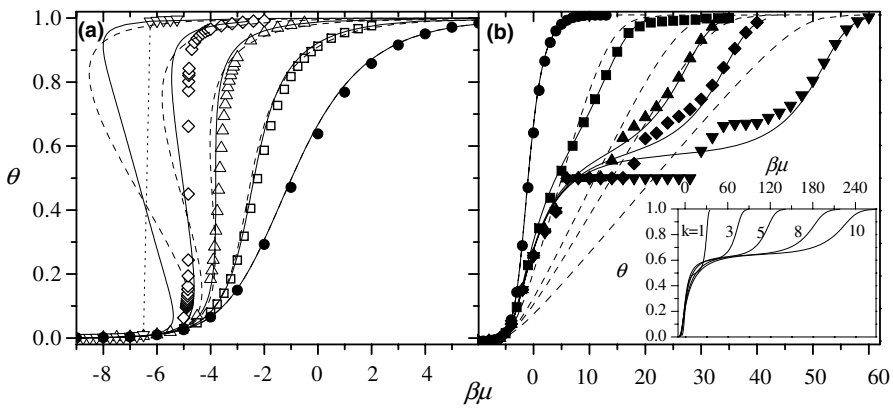

Fig. 6. Adsorption isotherms for homonuclear dimers adsorbed on a square lattice with nearest-neighbor interactions. Symbols, solid lines and dashed lines represent results from Monte Carlo simulations, QCA and BWA, respectively. The dotted lines are included in the figure as a guide for the eyes. (a) Attractive case: full circles, $\beta w = 0$; open squares, $\beta w = -0.5$; open up triangles, $\beta w = -1.0$; open diamonds, $\beta w = -1.4$ and open down triangles, $\beta w = -2.0$. (b) Repulsive case: full circles, $\beta w = 0$; full squares, $\beta w = 2.0$; full up triangles, $\beta w = 4.0$; full diamonds, $\beta w = 5.0$ and full down triangles, $\beta w = 7.5$. Inset: Adsorption isotherms from QCA for $\beta w = 7.5$ and different values of k as indicated.

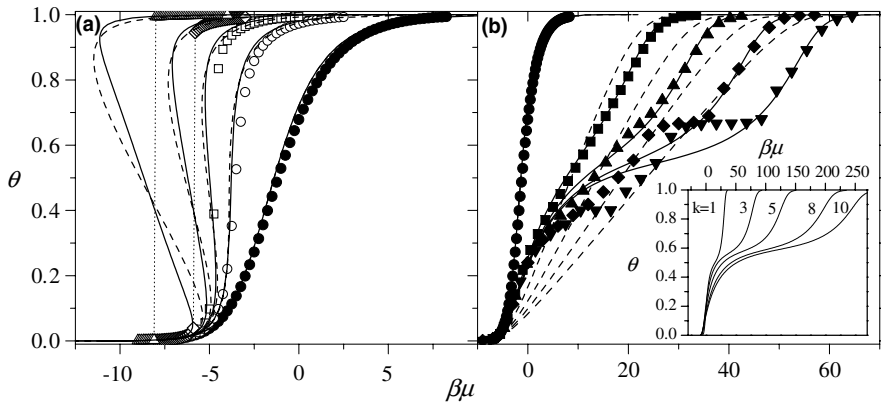

Fig. 7. Adsorption isotherms for homonuclear dimers adsorbed on a triangular lattice with nearest-neighbor interactions. Symbols, solid lines and dashed lines represent results from Monte Carlo simulations, QCA and BWA, respectively. The dotted lines are included in the figure as a guide for the eyes. (a) Attractive case: full circles, $\beta w = 0$; open circles, $\beta w = -0.5$; open squares, $\beta w = -0.75$; open diamonds, $\beta w = -1.0$ and open up triangles, $\beta w = -1.5$. (b) Repulsive case: full circles, $\beta w = 0$; full squares, $\beta w = 2.0$; full up triangles, $\beta w = 3.0$; full diamonds, $\beta w = 4.0$ and full down triangles, $\beta w = 5.0$. Inset: Adsorption isotherms from QCA for $\beta w = 5.0$ and different values of k as indicated.

the adsorbate: (1) a low-coverage ordered phase (LCOP), with 5/9, 1/2 and 2/5 of the sites occupied for honeycomb, square and triangular lattices, respectively; and (2) a high-coverage ordered phase (HCOP), with 2/3 of the sites filled for the three geometries. Snapshots corresponding to LCOP [part (a)] and HCOP [part (b)] for honeycomb, square and triangular lattices are shown in Figs. 8–10. For a more complete discussion of LCOP and HCOP, interested readers are referred to Refs. [54,55].

In the attractive cases, the two theoretical approximations agree qualitatively well and the adsorption isotherms for the BWA and QCA are hardly distinguishable from

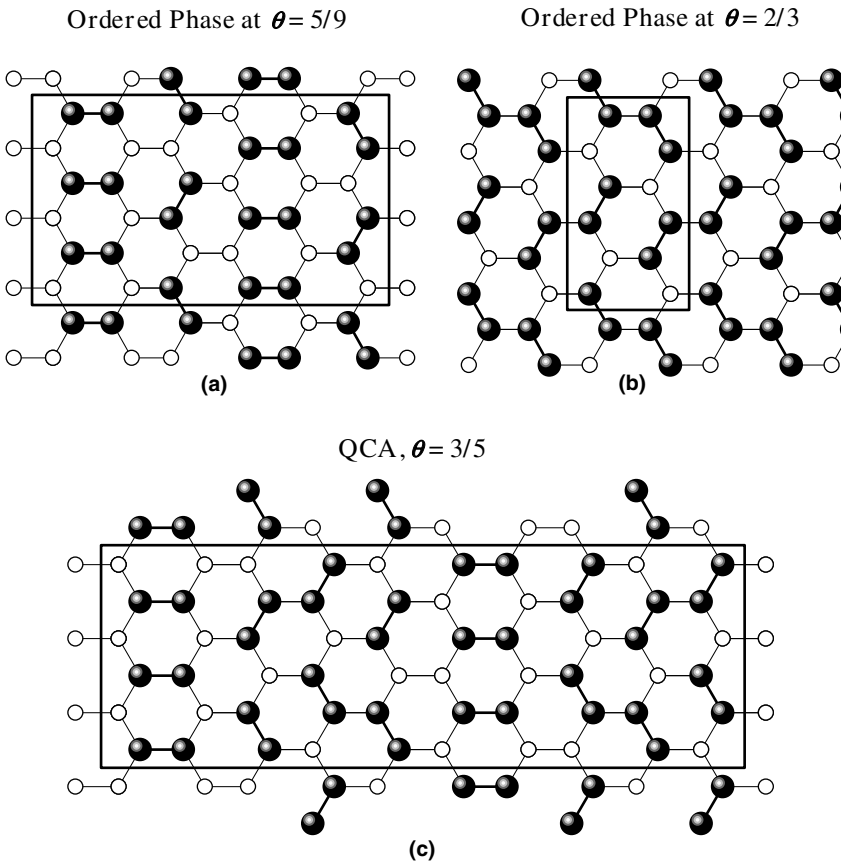

Fig. 8. Snapshots of the ordered phases corresponding to repulsive dimers adsorbed on a honeycomb lattice. (a) Low-coverage ordered structure (LCOP); (b) high-coverage ordered structure (HCOP) and (c) LCOP-HCOP mixture according to the predictions of QCA.

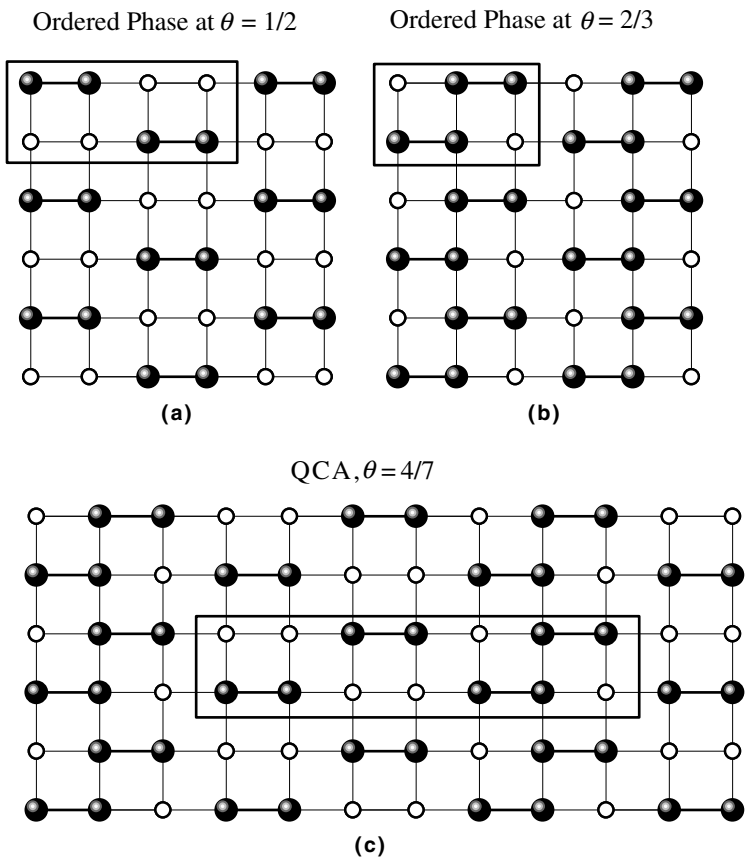

Fig. 9. As Fig. 8 for square lattices.

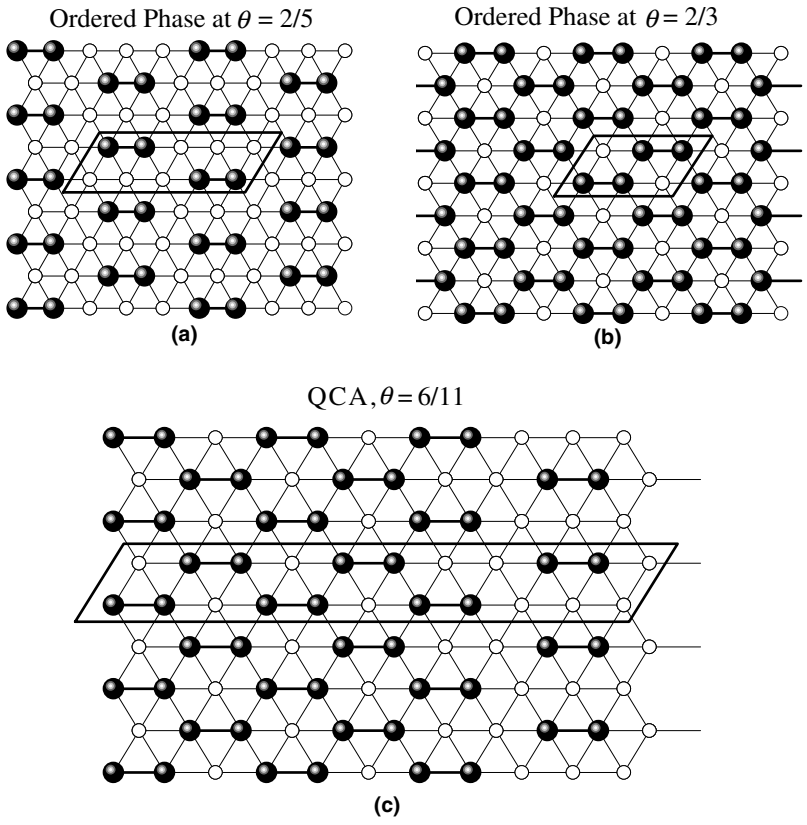

Fig. 10. As Fig. 8 for triangular lattices.

each other. However, it is known that the isotherms resulting from different approximations can look very similar [3]. The differences between numerical and theoretical results can be much easily rationalized with the help of the absolute error, $\varepsilon^{a}(\theta)$, which is defined as

$$\varepsilon^{a}(\theta) = |\mu_{theor} - \mu_{sim}|_{\theta}, \tag{43}$$

where μ_{sim} (μ_{theor}) represents the chemical potential obtained by using MC simulation (analytical approach). Each pair of values (μ_{sim}, μ_{theor}) is obtained at fixed θ.

As an example, Fig. 11(a) shows $\varepsilon^{a}(\theta)$ for three typical attractive cases: squares, $\beta w = -3.0$; triangles, $\beta w = -1.5$ and circles, $\beta w = -0.5$. Full and open symbols represent results from BWA and QCA, respectively. In all cases, QCA leads to appreciably better results than BWA. The curves in Fig. 11 correspond to a honeycomb lattice. However, the behavior of $\varepsilon^{a}(\theta)$ for square and triangular lattices is very similar (data are not shown here for sake of simplicity).

With respect to repulsive interactions, the differences between QCA and BWA are very appreciable. This situation is clearly reflected in Fig. 11(b), where three repulsive cases are depicted: squares, $\beta w = 8.0$; triangles, $\beta w = 4.0$ and circles, $\beta w = 2.0$. Full and open symbols are as in part (a).

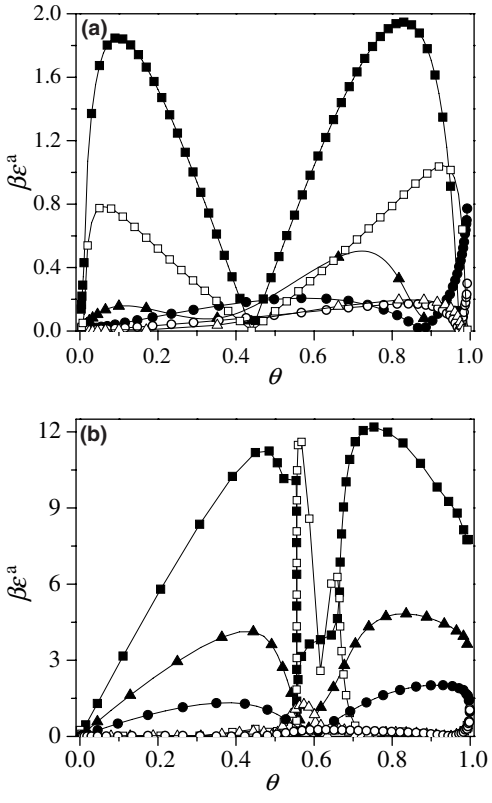

Fig. 11. Absolute error in $k_B T$ units, $\beta\varepsilon^{a}$, versus surface coverage for adsorption isotherms of dimers. The symbology is as follows: (a) Squares, $\beta w = -3.0$; triangles, $\beta w = -1.5$ and circles, $\beta w = -0.5$. (b) Squares, $\beta w = 8.0$; triangles, $\beta w = 4.0$ and circles, $\beta w = 2.0$. Full and open symbols correspond to comparisons with BWA and QCA, respectively.

Beyond the quantitative discrepancies between QCA and BWA, there exists qualitative differences between both approximations. Thus, while BWA does not predict the existence of ordered phases in the adsorbate, QCA isotherms present a pronounced plateau as the temperature lowers. This singularity or critical coverage θ_c^{QCA}, which appears at a intermediate coverage between the LCOP and the HCOP, depends on both the geometry of the substrate and the size of the adsorbate. The value of θ_c^{QCA} can be determined from the point of inflection in the adsorption isotherm equation (Eq. (29)), calculated in the limit as $\beta w \to \infty$. Thus,

$$\theta_c^{QCA} = \frac{(c/2)k}{(c-1)k+1}. \tag{44}$$

Fig. 12 shows the behavior of θ_c^{QCA} as a function of the k-mer's size, for the different connectivities studied. In the particular case of $k = 2$, $\theta_c^{QCA} = 3/5, 4/7$ and $6/11$, for honeycomb, square and triangular lattices, respectively. The configuration of the adsorbate at θ_c^{QCA} "could be thought" as a mixture of LCOP and HCOP [see part (c) in Figs. 8–10].

Summarizing, we define the integral error ε^{i}, which takes into account the differences between theoretical and simulation data in all range of coverage,

$$\varepsilon^{i} = \int_0^1 \varepsilon^{a}(\theta)\,d\theta. \tag{45}$$

The integral error is shown in Fig. 13 for all studied geometries and for a wide range of values of βw. Several conclusions can be drawn from the figure:

- In all cases, QCA gives a much better description of the MC adsorption isotherms than the BWA. In the particular case of repulsive interactions, the disagreement between MC and BWA turns out to be significantly

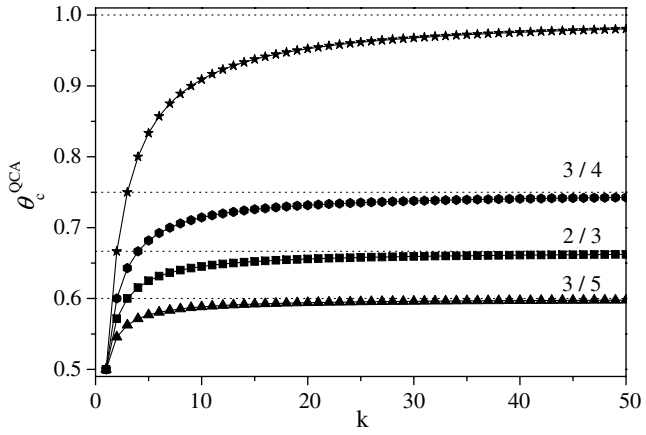

Fig. 12. Critical coverage θ_c^{QCA}, as a function of the adsorbate size k for different geometries: stars, one-dimensional lattices; hexagons, honeycomb lattices; squares, square lattices and triangles, triangular lattices.

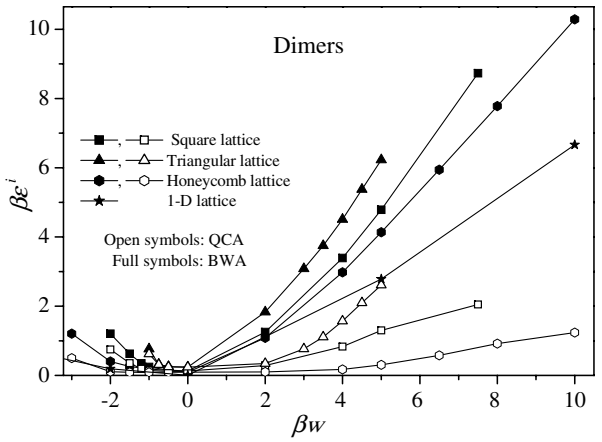

Fig. 13. Integral error in k_BT units, $\beta\varepsilon^i$, versus lateral interaction for different geometries as indicated.

large, while QCA appears as the simplest approximation capable to take into account the main features of the multisite occupancy adsorption.

- $\varepsilon^i(\theta)$ increases as the lattice connectivity is increased. A possible explanation for the deviation from QCA (and BWA) observed for high connectivity is associated with the choice of $g(N,M)$ in Eqs. (7) and (23). In fact, $g(N,M)$ is an extension to two dimensions of the exact configurational factor obtained in one dimension. Consequently, the accuracy of $g(N,M)$ diminishes as c is increased [35]. In the future, other expressions for $g(N,M)$ [35,36] will be investigated.
- There exists a wide range of βw's ($-1 \leqslant \beta w \leqslant 4$), where QCA provides an excellent fitting of the simulation data. In addition, most of the experiments in surface science are carried out in this range of interaction energy. Then, QCA not only represents a qualitative advance in the description of the adsorption k-mers with respect to the BWA, but also gives a framework and compact equations to consistently interpret thermodynamic adsorption experiments of polyatomics species such as alkanes, alkenes, and other hydrocarbons on regular surfaces.

We now analyze the behavior of the isosteric heat of adsorption. q_{st} versus coverage is plotted in Figs. 14–16, for honeycomb, square and triangular lattices, respectively. The curves are denoted as in Figs. 5–7.

The general features of the coverage dependence of the isosteric heat of adsorption for attractive k-mers are the following [see part (a) in Figs. 14–16]: q_{st} is monotonically increasing on coverage. As the ratio βw is increased, two main effects occur. (i) A plateau appears being $q_{st} = (c-1)w$. This behavior demonstrates that the island of adsorbed dimers grows through the perimeter, being $(c-1)w$, the involved energy in one adsorption–desorption

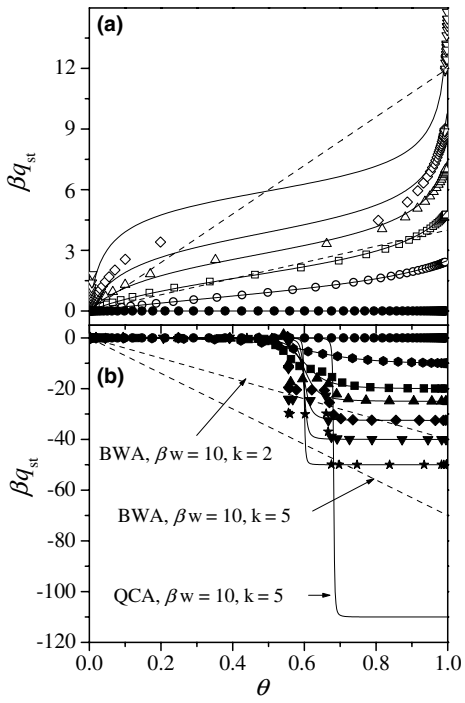

Fig. 14. Isosteric heat of adsorption in k_BT units, βq_{st}, versus surface coverage for attractive [part (a)] as well-repulsive [part (b)] interacting dimers and 5-mers adsorbed on a honeycomb lattice. The curves are labeled as in Fig. 5. In two limit cases ($\beta w = 10$, $k = 2$ and $\beta w = 10$, $k = 5$), the data are compared with BWA.

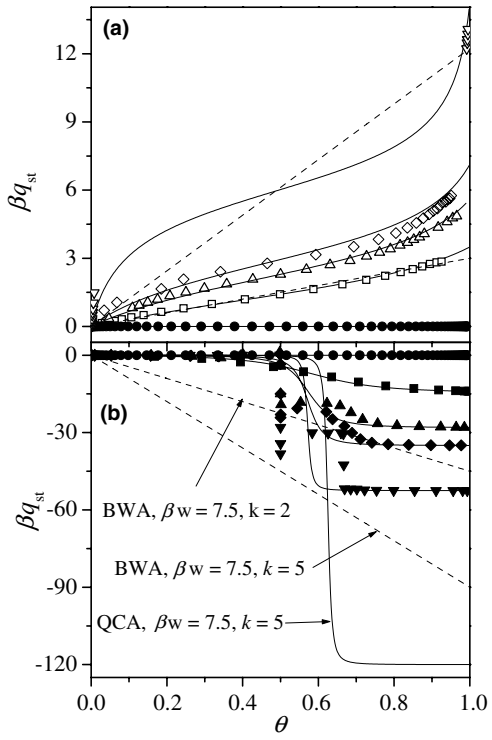

Fig. 15. Isosteric heat of adsorption in k_BT units, βq_{st}, versus surface coverage for attractive [part (a)] as well-repulsive [part (b)] interacting dimers and 5-mers adsorbed on a square lattice. The curves are labeled as in Fig. 6. In two limit cases ($\beta w = 7.5$, $k = 2$ and $\beta w = 7.5$, $k = 5$), the data are compared with BWA.

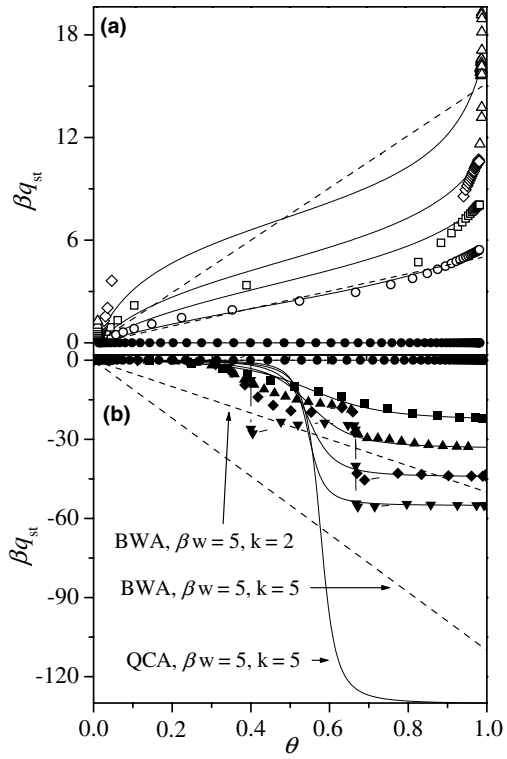

Fig. 16. Isosteric heat of adsorption in k_BT units, βq_{st}, versus surface coverage for attractive [part (a)] as well-repulsive [part (b)] interacting dimers and 5-mers adsorbed on a triangular lattice. The curves are labeled as in Fig. 7. In two limit cases ($\beta w = 5$, $k = 2$ and $\beta w = 5$, $k = 5$), the data are compared with BWA.

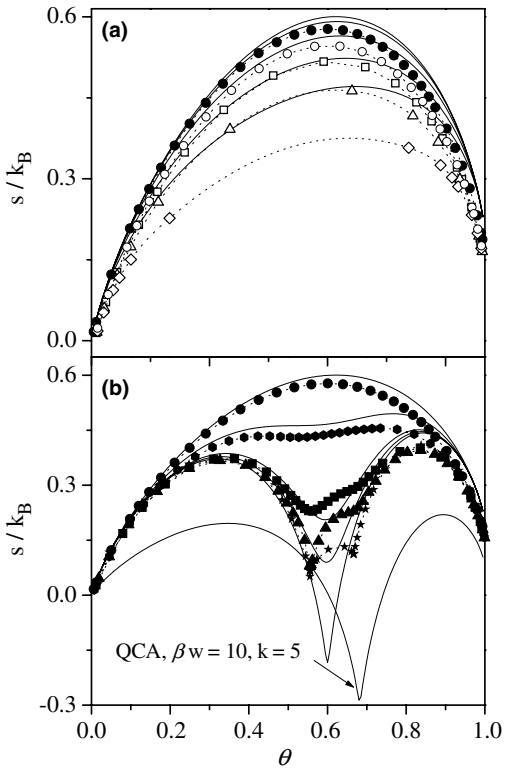

Fig. 17. Entropy per site as a function of coverage for homonuclear dimers and 5-mers adsorbed on a honeycomb lattice with nearest-neighbor interactions. The curves are labeled as in Fig. 5. (a) Attractive case and (b) repulsive case. Solid lines from top to bottom correspond one-to-one to the cases plotted with symbols. The dotted lines are included in the figure as a guide for the eyes.

of a dimer in the perimeter of the adsorbate island. (ii) The plateau flattens over a wide range of coverage since adsorbate islands are more compact for larger βw.

As it can be noticed, the differences between the theoretical approximations are notable. While QCA agrees very well with the curves of q_{st}, BWA presents a linear behavior and does not reproduce the main characteristics of q_{st}.

For the repulsive case [part (b) in Figs. 14–16], q_{st} varies from a smoothly decreasing (at high temperatures) to a double stepped function of θ (at low temperatures). The abrupt steps are traced to the presence of the ordered phases shown in Figs. 8–10. As in the attractive case, BWA varies linearly with the coverage and appears as a poor sensitive theory for studying q_{st}. On the other hand, even though QCA does not reproduce the two steps in the curves at very low temperatures, the approach agrees very well with the simulation data in a wide range of βw's and predicts the value of q_{st} at high coverage, $q_{st}(\theta \to 1)$. As it has been widely discussed in Refs. [43,55], the value of $q_{st}(\theta \to 1)$ can be only understood from reordering processes occurring in the adsorbate at high coverage, which do not appear in the case of monomers and, consequently, are a clear signal of the presence of multisite occupancy adsorption. These findings reinforce the validity of the proposed QCA to describe k-mers adsorption thermodynamics.

Finally, the behavior of the configurational entropy per site as a function of coverage is shown in Figs. 17–19. For attractive interactions [part (a) in Figs. 17–19], the overall behavior can be summarized as follows: for $\theta \to 0$ the entropy tends to zero. For low coverage, $s(\theta)$ is an increasing function of θ, reaches a maximum, then decreases monotonically. In the limit $\theta \to 1$ the entropy tends to a finite value, which is associated to the different ways to arrange the dimers at full coverage. This value depends on the geometry, being $s(\theta = 1)/k_B \approx 0.19$, 0.29 and 0.44 for $c = 3$, 4 and 6, respectively. The effect of the interactions is to decrease the entropy for intermediate coverage ($0 < \theta < 1$), remaining constant in the limits $\theta \to 0$ and $\theta \to 1$. The curves from QCA present a qualitative agreement with simulation data, but overestimate the value of the entropy in the whole range of θ.

In the case of repulsive interactions [part (b) in Figs. 17–19], s/k_B develops two minima as T decreases, corresponding to the presence of the LCOP and the HCOP. In the case of QCA, the curves present a minimum at θ_c^{QCA}. The value of $s(\theta = \theta_c^{QCA})/k_B$ decreases as βw is increased, reaching negative values for high βw's. This spurious behavior also appears in the classical QCA for monomers [1,2]. On the other hand and as it was discussed in Fig. 2, the entropy per site from BWA does not depend on βw.

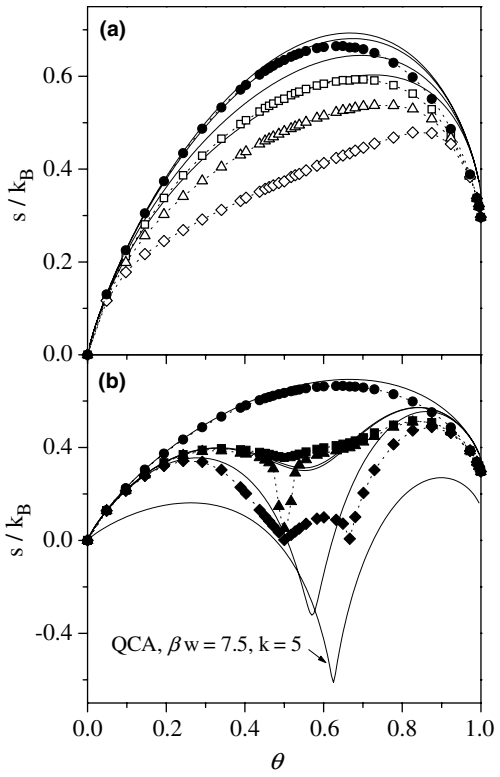

Fig. 18. Entropy per site as a function of coverage for homonuclear dimers and 5-mers adsorbed on a square lattice with nearest-neighbor interactions. (a) Attractive case: full circles, $\beta w = 0$; open squares, $\beta w = -0.5$; open up triangles, $\beta w = -1.0$ and open diamonds, $\beta w = -1.4$. (b) Repulsive case: full circles, $\beta w = 0$; full squares, $\beta w = 2.94$; full up triangles, $\beta w = 3.13$ and full diamonds, $\beta w = 7.5$. Solid lines from top to bottom correspond one-to-one to the cases plotted with symbols. The dotted lines are included in the figure as a guide for the eyes.

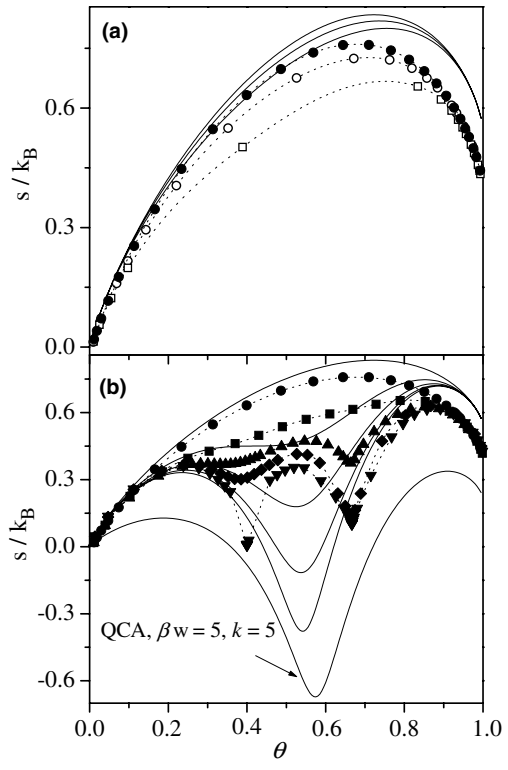

Fig. 19. Entropy per site as a function of coverage for homonuclear dimers and 5-mers adsorbed on a triangular lattice with nearest-neighbor interactions. The curves are labeled as in Fig. 7. (a) Attractive case and (b) repulsive case. Solid lines from top to bottom correspond one-to-one to the cases plotted with symbols. The dotted lines are included in the figure as a guide for the eyes.

4. Conclusions

A generalization of the quasi-chemical approximation for interacting polyatomic adsorbates on homogeneous surfaces has been presented. The main thermodynamic functions of adsorption (adsorption isotherm, configurational energy, isosteric heat of adsorption, specific heat and configurational entropy of the adlayer) have been calculated in the framework of the QCA and compared with analytical results from the classical Bragg–Williams approximation and MC simulation data for a lattice-gas of interacting dimers on one-dimensional, honeycomb, square and triangular lattices. The artificial effects that the BWA induces on the main thermodynamic functions can now be rationalized and compared with other analytical approaches.

The new formalism leads to exact results in one dimension and provides a close approximation to study adsorption of polyatomics on two-dimensional surfaces with different geometries (square, honeycomb and triangular).

From the comparison with MC simulations, appreciable differences can be seen for the different approximations, QCA being the most accurate for all cases.

In summary, the proposed theoretical model is simple, represents a qualitative advance with respect to the existing development on k-mers thermodynamics and seems to be a promising way toward a more accurate description of the adsorption thermodynamics of polyatomic molecules. In this sense, future efforts will be directed to (1) study the critical behavior of the system for attractive and repulsive interactions; (2) extend the calculations to kinetic properties as diffusion coefficient, thermal desorption; etc. and (3) consider different forms for $g(N, M)$ in Eqs. (7) and (23), analyzing its influence on the thermodynamic functions.

Acknowledgements

This work was supported in part by CONICET (Argentina) under project PIP 02425 and the Universidad Nacional de San Luis (Argentina) under the projects 328501 and 322000.

References

[1] T.L. Hill, An Introduction to Statistical Thermodynamics, Addison Wesley, Reading, MA, 1960.
[2] A. Clark, The Theory of Adsorption and Catalysis, Academic Press, New York/London, 1970.

[3] W.A. Steele, The Interaction of Gases with Solid Surfaces, Pergamon Press, New York, 1974.
[4] G. Rupprechter, M. Morkel, H.-J. Freund, R. Hirschl, Surf. Sci. 554 (2004) 43.
[5] T. Matsushima, Surf. Sci. 558 (2004) 1.
[6] K. Binder, D.P. Landau, Phys. Rev. B 21 (1980) 1941.
[7] D.P. Landau, Phys. Rev. B 27 (1983) 5604.
[8] A. Patrykiejew, S. Sokolowski, K. Binder, Surf. Sci. Rep. 37 (2000) 207.
[9] M. Plischke, B. Bergersen, Equilibrium Statistical Physics, Prentice Hall, New Jersey, 1989.
[10] N. Goldenfeld, Lectures on Phase Transitions and the Renormalization Group, Addison Wesley, Reading, MA, 1992.
[11] J.M. Yeomans, Statistical Mechanics of Phase Transitions, Clarendon Press, Oxford, 1992.
[12] E. Ising, Z. Physik 31 (1925) 253.
[13] C. Domb, in: C. Domb, M.S. Green (Eds.), Phase Transitions and Critical Phenomena, vol. 3, Academic Press, London/New York, 1974, p. 1;
M.E. Fisher, Rep. Prog. Phys. 30 (1967) 731.
[14] L. Onsager, Phys. Rev. 65 (1944) 117.
[15] H. Bethe, Proc. R. Soc. Lond. A 150 (1935) 552.
[16] W. Rudziński, D.H. Everett, Adsorption of Gases on Heterogeneous Surfaces, Academic Press, London, 1992.
[17] M. Tarek, R. Kahn, E. Cohen de Lara, Zeolites 15 (1995) 67.
[18] J.A.C. Silva, A.E. Rodrigues, Ind. Eng. Chem. Res. 38 (1999) 2434.
[19] F. Romá, J.L. Riccardo, A.J. Ramirez-Pastor, Langmuir 21 (2005) 2474.
[20] P. Zeppenfeld, J. George, V. Diercks, R. Halmer, R. David, G. Cosma, A. Marmier, C. Ramseyer, C. Girardet, Phys. Rev. Lett. 78 (1997) 1504.
[21] O.G. Mouritsen, A.J. Berlinsky, Phys. Rev. Lett. 48 (1982) 181.
[22] D. Ferry, J. Suzanne, Surf. Sci. 345 (1996) L19.
[23] J.W. He, C.A. Estrada, J.S. Corneille, M.C. Wu, D.W. Goodman, Surf. Sci. 261 (1992) 164.
[24] V. Panella, J. Suzanne, P.N.M. Hoang, C. Girardet, J. Phys. I 4 (1994) 905.
[25] D.L. Meixner, D.A. Arthur, S.M. George, Surf. Sci. 261 (1992) 141.
[26] H.N.V. Temperley, M.E. Fisher, Phil. Mag. 6 (1961) 1061.
[27] P.W. Kasteleyn, Physica 27 (1961) 1209.
[28] E.H. Lieb, J. Math. Phys. 8 (1967) 2339.
[29] A.J. Phares, F.J. Wunderlich, D.W. Grumbine, J.D. Curley, Phys. Lett. A 173 (1993) 365.
[30] P.J. Flory, J. Chem. Phys. 10 (1942) 51.
[31] P.J. Flory, Principles of Polymer Chemistry, Cornell University Press, Cornell, NY, 1953.
[32] M.L. Huggins, J. Chem. Phys. 46 (1942) 151;
Ann. NY Acad. Sci. 41 (1942) 151;
J. Am. Chem. Soc. 64 (1942) 1712.
[33] E.A. Guggenheim, Proc. R. Soc. Lond. A 183 (1944) 203.
[34] A.J. Ramirez-Pastor, T.P. Eggarter, V. Pereyra, J.L. Riccardo, Phys. Rev. B 59 (1999) 11027.
[35] F. Romá, A.J. Ramirez-Pastor, J.L. Riccardo, Langmuir 19 (2003) 6770.
[36] J.L. Riccardo, F. Romá, A.J. Ramirez-Pastor, Phys. Rev. Lett. 93 (2004) 186101.
[37] T. Nitta, M. Kuro-oka, T. Katayama, J. Chem. Eng. Jpn. 17 (1984) 45.
[38] J.L. Firpo, J.J. Dupin, G. Albinet, A. Bois, L. Casalta, J.F. Baret, J. Chem. Phys. 68 (1978) 1369.
[39] E.A. DiMarzio, J. Chem. Phys. 35 (1961) 658.
[40] G.L. Aranovich, M.D. Donohue, J. Colloid Interface Sci. 213 (1999) 457.
[41] S. Ono, S. Kondo, in: S. Flügge (Ed.), Molecular Theory of Surface Tension in Liquids, Encyclopedia of Physics, vol. 10, Springer, Berlin, 1960, p. 134.
[42] J. Des Cloizeaux, G. Jannink, Polymers in Solution: their Modelling and Structure, Clarendon Press, Oxford, 1990.
[43] A.J. Ramirez-Pastor, J.L. Riccardo, V. Pereyra, Langmuir 16 (2000) 10167.
[44] A.J. Ramirez-Pastor, A. Aligia, F. Romá, J.L. Riccardo, Langmuir 16 (2000) 5100.
[45] K. Binder (Ed.), Monte Carlo Methods in Statistical Physics, Topics in Current Physics, vol. 7, Springer, Berlin, 1978.
[46] D. Nicholson, N.D. Parsonage, Computer Simulation and the Statistical Mechanics of Adsorption, Academic Press, London, 1982.
[47] K. Binder (Ed.), Applications of the Monte Carlo Method in Statistical Physics, Topics in Current Physics, vol. 36, Springer, Berlin, 1984.
[48] N. Metropolis, A.W. Rosenbluth, M.N. Rosenbluth, A.H. Teller, E. Teller, J. Chem. Phys. 21 (1953) 1087.
[49] V.A. Bakaev, W.A. Steele, Langmuir 9 (1992) 148.
[50] F. Romá, A.J. Ramirez-Pastor, J.L. Riccardo, Phys. Rev. B 72 (2005) 035444.
[51] F. Romá, A.J. Ramirez-Pastor, J.L. Riccardo, Langmuir 16 (2000) 9406.
[52] F. Romá, A.J. Ramirez-Pastor, J.L. Riccardo, J. Chem. Phys. 114 (2001) 10932.
[53] F. Rittner, B. Boddenberg, M.J. Bojan, W.A. Steele, Langmuir 15 (1999) 1456.
[54] A.J. Ramirez-Pastor, J.L. Riccardo, V. Pereyra, Surf. Sci. 411 (1998) 294.
[55] J.E. González, A.J. Ramirez-Pastor, V.D. Pereyra, Langmuir 17 (2001) 6974.